

9.5 12GHz Low-Area-Overhead Standing-Wave Clock Distribution with Inductively-Loaded and Coupled Technique

Mamoru Sasaki¹, Mitsuru Shiozaki¹, Atsushi Mori¹, Atsushi Iwata¹, Hiroaki Ikeda²

¹Hiroshima University, Hiroshima Japan

²Elpida Memory, Kanagawa Japan

Global clock distribution is becoming increasingly difficult for multi-GHz microprocessors, because skew and jitter are proportional to latency, which does not scale with the clock period for a conventional tree structure. Furthermore, the clock is the most active signal, thus the clock power dominates the total power consumption. Some resonant techniques have been proposed to overcome these clock distribution problems [1,2]. The left of Fig. 9.5.1 illustrates two standing-wave oscillators: a long transmission line (TL) grounded at both ends and a short TL with two inductors. The long TL has the conventional standing-wave-resonance mode and the first resonant standing-wave is illustrated in the figure. The short TL has an interesting standing wave that cuts the low-amplitude segment away compared with the conventional one, as shown in Fig. 9.5.1, although the resonance frequency is identical in both cases [3]. The standing wave has uniform-phase and almost uniform-amplitude. As shown on the right of Fig. 9.5.1, clock distribution is achieved with a fine grid mesh, and the depth of the clock tree becomes very shallow. This results in small latency, low jitter and low skew. However, the mesh structure has a spiral inductor and a MOSFET cross-coupled pair (not shown) at every grid point, which is one factor that increases the area overhead.

To overcome this drawback, we propose a new mesh structure of standing-wave oscillators. In the structure, shown in Fig. 9.5.2, the inductors are magnetically coupled to each other by mutual inductance, M , at the end of the TL composing the oscillators. Magnetic coupling synchronizes the standing wave oscillations. As described in Fig.9.5.2, the synchronized oscillation frequency, f_{ck} , is expressed by almost the same equation as for a single inductively loaded standing wave oscillator [3]. Z_0 is the characteristic impedance and β is phase constant of the TL; k ($= M/L$) is the coupling coefficient between the inductors. Figure 9.5.2 shows a low-area-overhead clock-distribution network with inductively coupled standing wave oscillators. In the network, the standing wave oscillators are placed in rows and columns and they are inductively coupled in circular form. This results in a mesh structure; however, there is no electrical contact at any grid point. Spiral inductors and MOSFET cross-coupled pairs (not shown) surround the mesh structure. Compared with the previous mesh structure of Fig. 9.5.1, the coupling technique and elaborate placement of oscillators reduces the area overhead caused by spiral inductors and MOSFET cross-coupled pairs. The reduction becomes more effective as the grid pitch becomes finer and the grid size becomes larger. Clock buffers are uniformly distributed on the TL, as shown in Fig. 9.5.2. In this case, the same design method can be adopted by modifying the distributed TL unit capacitance, ΔC , into $\Delta C + (nC_{buf})/l$, where, C_{buf} is the input capacitance and n is the number of the clock buffers. The oscillation starts as follows. Immediately after power is supplied, many oscillation modes having small amplitude appear; however, only stable oscillation is developed from these oscillation modes. Fortunately, with regard to the fundamental frequency, the stable mode is unique as described above.

A 12GHz magnetically-coupled standing-wave clock-distribution network is prototyped in 0.18 μ m CMOS with 6 Al metal layers. Figure 9.5.7 shows a micrograph of the prototype integrated in a 5 \times 5 mesh clock-distribution network. The TL is configured as a coplanar structure with the 6th metal layer, and the power and

ground lines are placed under the TL in the 1st and 2nd metal layers. The width and space of the coplanar structure are 5 and 2 μ m, respectively. The inductor is implemented as a spiral inductor with the 5th and 6th metal layers, and is magnetically coupled to the adjacent inductors on both sides by the stacked structure, as illustrated in Fig. 9.5.7. The outside diameter and internal diameter of the spiral inductor are 70 and 50 μ m, respectively. The TL has 2 spiral inductors at each end and they are connected to respective differential lines. A simple NMOS cross-coupled pair, shown in Fig. 9.5.7, is employed and is placed between the 2 spiral inductors. The power supply of 0.9V is supplied through the spiral inductors. The transistor size is 1.2 μ m/0.18 μ m, and the finger count is 20. For the measurements, ground-signal-signal-ground (G-S-S-G) pads are placed on the outside of the mesh network, and the signal pads are capacitively coupled to the differential TL. The measured attenuation of the capacitively coupled pad is -21dB at 11.5GHz. Attenuation minimizes the probing influence on the TL [3].

Fig. 9.5.3 shows the measured spectrum as the 11.5GHz clock oscillates on the 5 \times 5 mesh clock distribution network. The measured phase noise at an offset of 1MHz is -103dBc/Hz, as shown in Fig. 9.5.4, and the rms clock jitter (calculated from the phase noise) is 0.86ps. Figure 9.5.5 shows the oscillation waveform with a period of 86.1ps, and peak-peak jitter of 4.7ps and rms jitter of 0.81ps. The measured rms jitter is in agreement with the rms jitter calculated from the phase noise. The peak-to-peak jitter is 5.5% of the clock period. For the measurement, an oscillation swing of 0.6Vpp is attained by calibration with the -21dB attenuation of the capacitively-coupled pad. The power consumption is 80mW at a supply voltage of 0.9V. The length of the TL is 1mm, which is 1/3 the length of the conventional standing-wave oscillator [1]. The mesh pitch is 200 μ m, achieved by elaborate placement of the inductively coupled standing-wave oscillators. The supply voltage to the oscillator defines the central voltage of the oscillation wave and can be tuned to the threshold voltage of the inverters by an on-chip regulator. The 0.6V_{pp} swing is sufficient for compensation of the mismatch in the threshold voltage among the inverters, therefore is possible to use simple inverters as the clock buffers.

In the time domain measurement, two wafer probes are placed on the different G-S-S-G pads, and one signal is measured by an equivalent sampling oscilloscope, using another signal as the trigger. The time-domain waveforms are measured for any combination of the two signals. Thus, all standing wave oscillators are synchronized with regard to the clock frequency. The phase properties are shown in Fig. 9.5.6. Four measured clock waves are superimposed in Fig. 9.5.6. The skew is less than 8ps and this is 9.6% of the clock period.

References:

- [1] F. O'Mahony, C.P. Yue, M.A. Horowitz, and S.A. Wong, "10GHz Clock Distribution Using Coupled Standing-Wave Oscillators," *ISSCC Dig. Tech. Papers*, pp. 428-429, Feb., 2003.
- [2] S.C. Chan, K.L. Shepard, and P.J. Restle, "Uniform-Phase Uniform-Amplitude Resonant-Load Global Clock Distributions," *J. Solid-State Circuits*, vol. 40, no. 1, pp. 102-109, Jan., 2005.
- [3] M. Sasaki, M. Shiozaki, A. Mori, et al., "17GHz Fine Grid Clock Distribution with Uniform-Amplitude Standing-Wave Oscillator," *Symp. VLSI Circuits*, pp. 124-125, Jun., 2006.

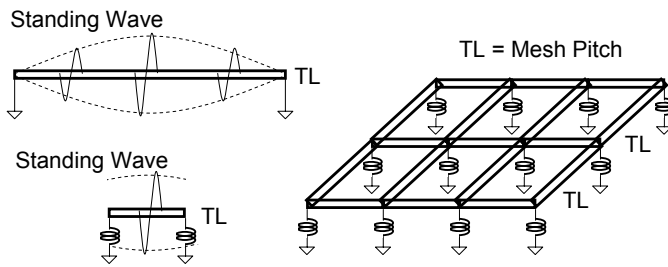


Figure 9.5.1: Inductively-loaded standing-wave oscillator.

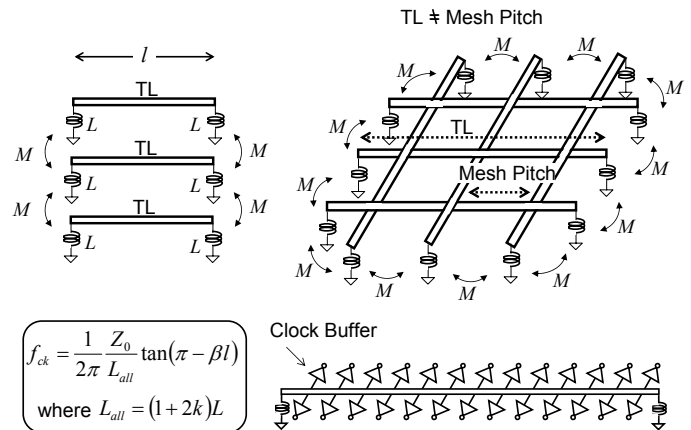


Figure 9.5.2: Magnetic coupling synchronization.

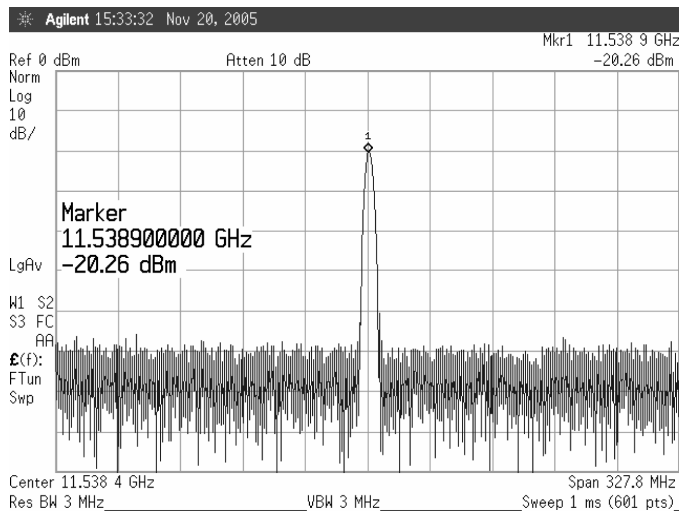


Figure 9.5.3: Measured frequency spectrum.

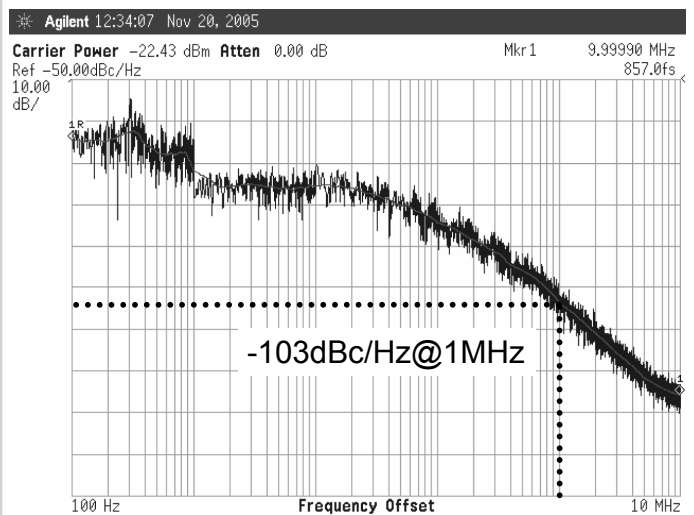


Figure 9.5.4: Measured phase noise.

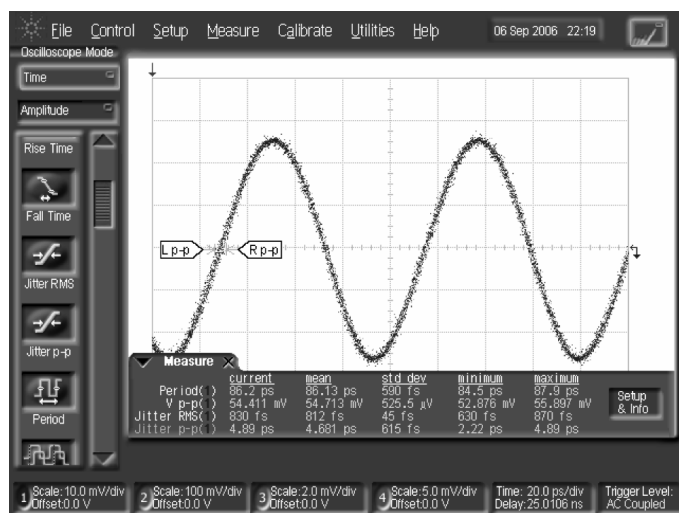


Figure 9.5.5: Measured oscillation waveform.

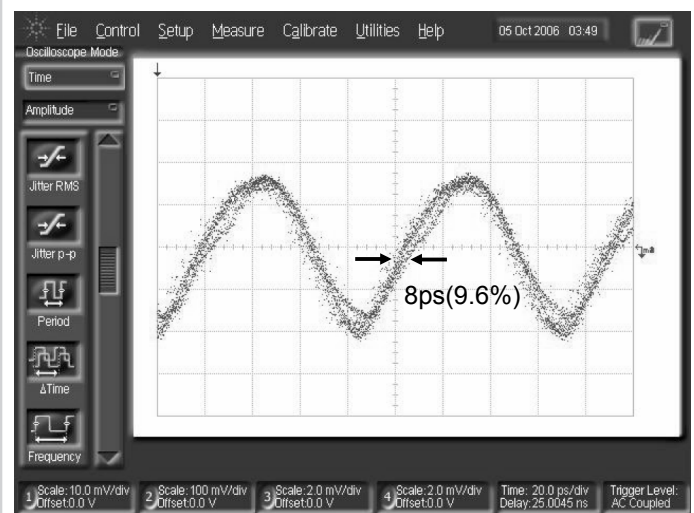


Figure 9.5.6: Measured phase properties.

Continued on Page 595

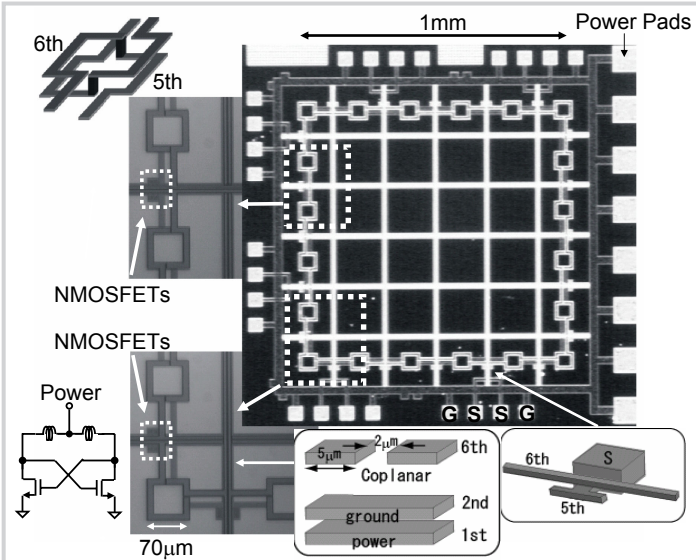


Figure 9.5.7: Micrograph of the prototype chip.